A High-Na^+ Conduction State during Recovery from Inactivation in the K^+ Channel Kv1.5

Zhuren Wang, J. Christian Hesketh, and David Fedida
Department of Physiology, University of British Columbia, Vancouver, British Columbia V6T 1Z3, Canada

ABSTRACT Na^+ conductance through cloned K^+ channels has previously allowed characterization of inactivation and K^+ binding within the pore, and here we have used Na^+ permeation to study recovery from C-type inactivation in human Kv1.5 channels. Replacing K^+ in the solutions with Na^+ allows complete Kv1.5 inactivation and alters the recovery. The inactivated state is nonconducting for K^+ but has a Na^+ conductance of 13% of the open state. During recovery, inactivated channels progress to a higher Na^+ conductance state (R) in a voltage-dependent manner before deactivating to closed-inactivated states. Channels finally recover from inactivation in the closed configuration. In the R state channels can be reactivated and exhibit supernormal Na^+ currents with a slow biexponential inactivation. Results suggest two pathways for entry to the inactivated state and a pore conformation, perhaps with a higher Na^+ affinity than the open state. The rate of recovery from inactivation is modulated by Na^+_o such that 135 mM Na^+_o promotes the recovery to normal closed, rather than closed-inactivated states. A kinetic model of recovery that assumes a highly Na^+-permeable state and deactivation to closed-inactivated and normal closed states at negative voltages can account for the results. Thus these data offer insight into how Kv1.5 channels recover their resting conformation after inactivation and how ionic conditions can modify recovery rates and pathways.

INTRODUCTION

Voltage-gated K^+ channels (Kv channels) activate and open upon membrane depolarization. In response to prolonged or repetitive depolarization most Kv channels exhibit a variable-speed (C-type) inactivation (Grissmer and Cahalan, 1989; Hoshi et al., 1991; Yellen et al., 1994), in which channels enter an inactivated state and as a result lose their K^+ conductance but become more permeable to Na^+ ions (Starkus et al., 1997; Kiss et al., 1999). A great deal has been learned recently about the processes involved in C-type inactivation. A current hypothesis proposes that C-type inactivation involves a constriction within the outer mouth of the pore resulting from a cooperative conformational change of the channel subunits (Ogielska et al., 1995; Panyi et al., 1995; Liu et al., 1996; Loots and Isacoff, 1998). This rearrangement of the outer mouth of the pore greatly reduces the conductance of K^+ relative to the conductance of Na^+, altering the ion selectivity of the channel (Starkus et al., 1997). Recently it has been further proposed that during C-type inactivation the channels dwell in at least three conformational states: an initial open state that is highly selective for K^+, a state that is less permeable to K^+ and more permeable to Na^+, and then a state that is nonconducting (Loots and Isacoff, 1998; Kiss et al., 1999).

When K^+ channels are in the open state, they are all very selective for K^+ rather than Na^+, such that relatively small amounts of intracellular K^+ can exclude Na^+ permeation. For this reason, only a few native channels have been demonstrated to conduct Na^+, like delayed rectifier K^+ channels in sympathetic and dorsal root ganglion neurons (Zhu and Ikeda, 1993; Callahan and Korn, 1994; Block and Jones, 1996) and the squid axon under extreme conditions (Bezanilla and Armstrong, 1972; French and Wells, 1977). This has changed a great deal with the work of Ikeda and Korn on cloned channels (Korn and Ikeda, 1995; Kiss et al., 1998), which shows that Kv2.1 has a significantly higher Na:K conductance ratio than Kv1 channels (Kv1.5 and Kv1.3). *Shaker* channels seem to have a much lower relative Na^+ conductance (Ogielska and Aldrich, 1998; Kiss et al., 1999) unless specific chimeric forms or point mutants are used (e.g., A463C in *Shaker*). On the other hand, *Shaker* channels show a remarkable Na^+ and Li^+ conductance of the inactivated state (Starkus et al., 1997, 1998), which can be seen as a sustained current during prolonged depolarization or as slow tails on deactivation. In Kv1.5, a transient Na^+ conductance can be seen that inactivates almost completely, with a residual current of less than 15% of peak current that represents Na^+ flux through inactivated channels. However, a striking observation in Kv1.5 channels is that repolarization to negative voltages generates slow Na^+ tail currents with a very prominent initial rising phase followed by the slow decay observed in *Shaker* channels. Here we demonstrate that on repolarization the inactivated channels initially increase their Na^+ conductance. The results provide evidence that at negative potentials the inactivated channels enter a state different from the open state that is more permeable to Na^+ and in which K^+ conductance is still prevented. An increase in external Na^+ can promote recovery to normal closed states, suggesting that Na^+ and/or K^+ binding to external site(s) could facilitate the recovery from inactivation.

Received for publication 10 February 2000 and in final form 18 July 2000.
Address reprint requests to Dr. David Fedida, Department of Physiology, University of British Columbia, 2146 Health Sciences Mall, Vancouver, BC V6T 1Z3, Canada. Tel.: 604-822-5806; Fax: 604-822-6048; E-mail: fedida@interchange.ubc.ca.

0006-3495/00/11/2416/18 $2.00

We propose that full recovery from C-type inactivation in Kv1.5 involves a multistate pathway in which the channels initially enter an intermediate state (R) that is more permeable to Na^+ and impermeable to K^+, and then deactivate to closed inactivated states and closed noninactivated states. The entry to the R state is necessary for the recovery of inactivated channels. Increasing external Na^+ and K^+ facilitates recovery from inactivation by promoting channel deactivation to normal closed states. In human heart, Kv1.5 is active during atrial action potential repolarization (Fedida et al., 1993) and is present in significant amounts in both human (Mays et al., 1995) and rat (Dixon and McKinnon, 1994; Barry et al., 1995) ventricular muscle. Modulation of recovery of the inactivated channels will vary the number of channels available with each beat and, as a result, may have important effects on action potential repolarization, duration, and, therefore, contractility.

MATERIALS AND METHODS

Cells and solutions

Human Kv1.5 channels stably expressed in HEK-293 cell lines were used in all experiments. Kv1.5 in the plasmid expression vector pCDNA3 was mutagenized using the Quickchange Kit (Stratagene, La Jolla, CA) to convert Arg^{487} to Val (R487V). HEK-293 cells were stably transfected with wild-type (WT) hKv1.5 or Kv1.5-R487V cDNAs using LipofectACE reagent (Canadian Life Technologies, Bramalea, ON, Canada) in a 1:10 (w/v) ratio. Patch pipettes contained (in mM) 135 NaCl, 5 EGTA, and 10 HEPES, adjusted to pH 7.2 with NaOH. When NaCl was replaced with KCl or *N*-methyl D-glucamine (NMG^+), pH was adjusted with KOH or HCl, respectively. The bath solution contained (in mM) 135 NMG^+, 5 NaCl, 10 HEPES, 1 $MgCl_2$, 1 $CaCl_2$, adjusted to pH 7.4 with HCl. For recordings in the presence of different external Na^+ or K^+ concentrations, the NMG^+ base external solution was used, and the concentration of NMG^+ was reduced as the cation concentration was elevated to maintain constant osmolarity. Throughout the text the subscripts i and o denote, respectively, intra- or extracellular ion concentrations. All chemicals were from Sigma Aldrich Chemical Co. (Mississauga, ON, Canada). The purity of the *N*-methyl D-glucamine was 99–100.5% (by HCl titration, M2004). All water used in these experiments was passed through organic filters and two-stage distillation before it was pssed through a Milli-Q (Millipore, Etobicoke, ON, Canada) deionizing system that returned water with a resistance of ~20 MΩ. The contaminating K^+ in the water used for solutions was below detection limits (<0.25 μM) for coupled plasma optical emission spectroscopy (CANTEST Analytical Services, Vancouver, BC, Canada), and a 140 mM NMG^+ solution also had undetectable levels of K^+. The 135 mM Na^+ solution gave a reading of 9.5 μM K^+, which was due to interference by the high Na^+ concentration.

Electrophysiological procedures

Coverslips containing cells were removed from the incubator before experiments and placed in a superfusion chamber (volume 250 μl) containing the control bath solution at 22–23°C. The bath solution was exchanged by switching the perfusates at the inlet of the chamber, with complete bath solution changes taking 5–10 s. Whole-cell current recording and data analysis were done using an Axopatch 200A amplifier and pClamp6 software (Axon Instruments, Foster City, CA). Patch electrodes were fabricated using thin-walled borosilicate glass (World Precision Instruments, Sarasota, FL). Capacity compensation was routinely used (the averaged cell membrane capacitance was 15.4 ± 0.3 pF, $n = 126$), but series resistance (R_s) compensation was only used in recording K^+ currents. Measured series resistance was between 1 and 3 MΩ for all recordings (the averaged series resistance was 2.18 ± 0.05 MΩ, $n = 126$). When this changed during the course of an experiment, data were discarded. No difference between results with and without R_s compensation was observed when we recorded Na^+ currents. Data were sampled at 10–20 kHz and filtered at 5–10 kHz. The data for analysis and presentation were off-line leak subtracted if required, and data were discarded if the leakage conductance was greater than 1 nS. During analysis, we measured the instantaneous tail current as soon as possible after the voltage clamp had settled, usually <200 μs after the end of a repolarizing voltage step. Throughout the text data are shown as mean ± SE. In Figs. 4 and 7 the apparent voltage sensitivity of transitions in deactivation or inactivation pathways was obtained by fitting τ-V curves to the relationship $\tau(V) = \tau(0)\exp(\pm Vq/kT)$, where V, k, and T have their usual meanings and q is the apparent charge moved for the transition in question (Starkus et al., 1997).

Formulation of the model

The model was constructed using SCoP and SCoPfit, version 3.51 (Simulation Resources, Redlands, CA). The number of channels moving between different states was described by a series of first-order differential equations and solved numerically. Opening of the channel from negative potentials is assumed to follow a standard linear scheme involving initial transitions between closed states (denoted as C_n). These rates were determined from a gating current model published previously (Hesketh and Fedida, 1999). The final opening transition from state C4 to the open state (O) proceeds with a relatively voltage-independent rate obtained from a previously published model of Kv1.5 ionic currents (DeBiasi et al., 1997). In the presence of sodium (and the absence of potassium), the channel rapidly enters the inactivated state (I) from the open state. The sustained current during depolarizations greater than 200 ms implies that the inactivated state conducts sodium current, but with a conductance much lower than that of the open state. We assume that essentially 100% of channels inactivate on depolarization, from the lack of a fast tail current on repolarization after intermediate duration depolarizations (e.g., Fig. 1 *C*).

RESULTS

The most striking feature of Na^+ permeation through K^+ channels is the rapid C-type inactivation that is present when channels are open at depolarized potentials (Starkus et al., 1997; Kiss and Korn, 1998; Ogielska and Aldrich, 1999) (Fig. 1). Kv1.5 is no exception to this, as although a slow inactivation process is present in Kv1.5 when physiological pipette and bath solutions are used (Fig. 1 *A*, 135 K_i^+/5 K_o^+), replacement of the K^+ with Na^+ results in currents that are much more rapidly inactivating (Fig. 1 *B*). An envelope of tails test confirms that the Na^+ currents through Kv1.5 inactivate in a classical C-type manner. In this situation, the magnitude of the deactivating tail currents should be proportional to the current activated during the depolarizing pulses that elicited those tails (Hodgkin and Huxley, 1952). Fig. 1 *C* shows current recordings in symmetrical 135 mM Na^+ at +80 and tails at −80 mV to allow a direct comparison of outward and inward current amplitudes. Even for short-duration depolarizations (20 ms), the Na^+ tail currents show an initial transient inward phase with fast kinetics of decay and then a rising phase followed by a slower second

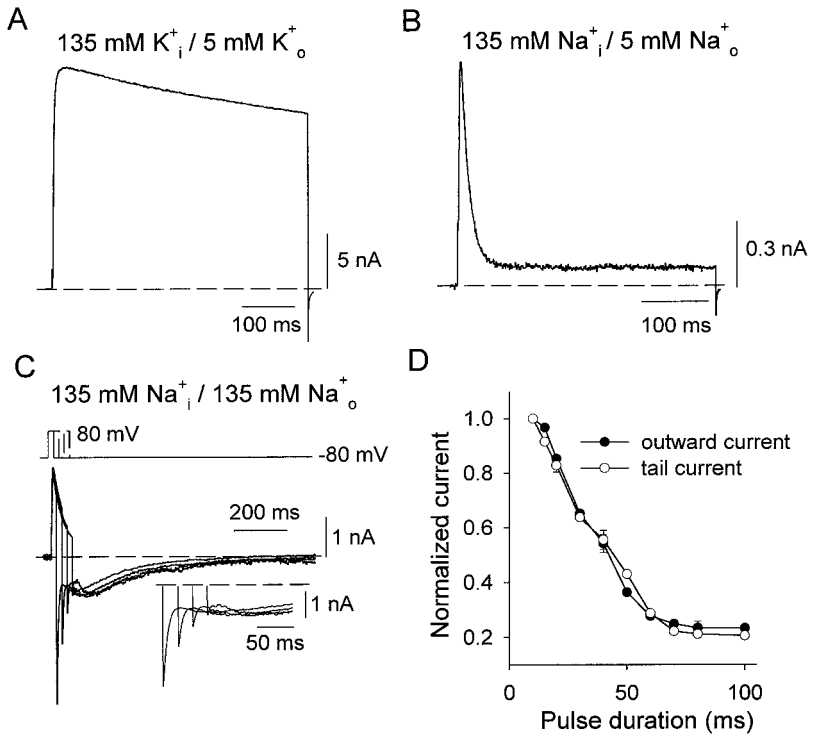

FIGURE 1 Rapid C-type inactivation in Na^+-conducting Kv1.5 channels. (*A*) 135 mM K_i^+/5 mM K_o^+. The current was recorded at +60 mV for 500 ms from −80 mV. (*B*) 135 mM Na_i^+/5 mM Na_o^+. As in *A*, but for 400 ms. (*C*) Symmetrical 135 mM Na_I^+/Na_o^+. The pulse protocol is shown at the top. An initial 20-ms depolarization was given from −80 to +80 mV and incremented by 20 ms for each subsequent pulse, given every 20 s. Note that with increasing test pulse duration, the initial fast tail was progressively reduced, as the rising phase became apparent. Enlarged tail currents are shown in the inset. (*D*) Normalized outward currents at the end of depolarizing pulses (●) and instantaneous tail currents (○) as functions of pulse duration from data as in *C*. Data represent mean ± SE (n = 5). In this figure, as in all others, dotted lines represent zero current.

phase of current decay. With longer duration and increased inactivation, the fast initial tail is quickly reduced, as the rising phase predominates (Fig. 1 *C, inset*). The large transient tail currents after brief depolarizations reflect the deactivation of open channels and get smaller with a time course similar to that of the decay of outward conductance, i.e., they both reflect development of inactivation. Mean normalized outward currents or peak tail amplitudes form identical relationships when plotted against the duration of depolarization (Fig. 1 *D*). The fast component of tail decay reflects deactivation of activated channels, and the reduction of this component, which parallels the decay of outward current, supports the idea of rapid C-type inactivation of Na^+ currents through activated Kv1.5 channels. As the time course of tail current decrease in Fig. 1 *D* is monotonic, along with the decay of outward conductance, it appears that inactivation proceeds from the open state to a single absorbing state in Kv1.5 with symmetrical Na_i^+/Na_o^+.

Intrinsically *Shaker* channels can inactivate within microseconds (Lopez-Barneo et al., 1993), and the process is delayed or prevented by the presence of ions bound at sites within or close to the permeation pathway (Starkus et al., 1997). Ions like Na^+ with a shorter dwell time (than K^+) at these sites are less able to prevent the onset of inactivation. Not only is the time course of inactivation accelerated, but the inactivation is more complete for Na^+ compared with K^+ currents, which are inactivated by only ~60% in Kv1.5 (Fedida et al., 1999).

In *ShD*Δ channels, transient outward Na^+ currents are followed by a sustained current that is ~50% of the peak (Starkus et al., 1997). This sustained current is due to Na^+ ions passing through inactivated channels. In Kv1.5, sustained Na^+ currents through inactivated channels could be observed with prolonged depolarization (Fig. 1 *B*). However, the amplitude of the sustained current in Kv1.5 is smaller than that in *Shaker* channels, so that at the end of 1-s depolarizing pulses, the current is 0.13 ± 0.02 (n = 6) of the peak current. In symmetrical Na^+ there is no evidence that, during the onset of inactivation, Kv1.5 channels enter a state of higher Na^+ conductance before reaching a state of relatively low Na^+ conductance (Fig. 1 *C*). This would have been seen in the envelope of tails test as an initial increase in peak inward tail current amplitude before its subsequent decay (see Discussion).

Increased Kv1.5 Na^+ conductance during the recovery from C-type inactivation

The significant features of the slow Na^+ tail currents observed in Fig. 1 *C* are the initial rising phase and the subsequent slow decay that lasts between 1.0 and 1.5 s. The slow decay of Na^+ tail currents was observed in *ShD*Δ channels, and it was suggested that this represented the deactivation of C-type inactivated channels to closed inactivated states (Starkus et al., 1997). However, the clear rising phase of Na^+ tail currents in Kv1.5 was a less

prominent feature in *Sh*Δ and so has not been investigated in detail. Investigation of the rising phase of the tail current forms the primary subject of this paper. On repolarization, current develops in the inward direction to form a "hook" before slowly decaying to the zero current level. The inward current reaches a peak within ~200 ms, and the slow decay is almost complete over the next 1.5 s or so.

A classical double-pulse protocol, which is often used to evaluate the time course of recovery from inactivation, clearly reveals the presence of this state of increased Na^+ conductance (Figs. 2 and 3). In symmetrical Na^+, a 400-ms prepulse to +60 mV drives the channels to the inactivated state, and then a test pulse after increasing repolarization intervals tests the fraction of available channels. Test pulses elicit an outward current that increases in peak amplitude rapidly at short repolarization intervals (Fig. 2 *A*). These outward currents, at pulse intervals of ≤1 s, inactivate significantly more slowly than currents during the prepulse. Clearly, the slowest decay of current during the test pulses is seen for that elicited near the peak of the inward tail current. This suggests that during the rising phase of slow inward tail currents, the channel conformation is different from that in the open state (Fig. 2 *A* and Fig. 3; see below). At longer repolarization intervals, recovery of peak current progresses with a slower exponential time course (Fig. 2 *B*), and the current decay during test pulses speeds up (not shown). The overall biexponential recovery of current amplitude is shown in Fig. 2 *C* as the filled points and solid line. A rapid phase of recovery with a time constant of ~1 s is followed by a slower recovery phase, which is complete by 20 s. Superimposed on the recovery relation is a second relation (*dotted line*) obtained in 135 mM Na_i^+/5 mM Na_o^+. This relation is described in more detail in Fig. 3 but is shown here to illustrate a clearer separation of the different phases of recovery from inactivation. The increased Na^+ conductance early after repolarization results in a novel "double peak" recovery relation that is quite different from the classical single or double exponential uninterrupted recovery from inactivation seen in K^+-containing solutions (Fedida et al., 1999; Rich and Snyders, 1998) or with symmetrical Na^+ solutions (Fig. 2).

Although the slow tail currents are invisible on repolarization to −80 mV in 5 mM Na_o^+ because of the small driving force, channels still appear to follow a qualitatively similar pathway. This is illustrated in Fig. 3 *A*, where Na_i^+ was replaced by NMG_i^+. Little outward current is seen, but the rising phase and slow decay of the inward tail after repolarization are clear. In the double-pulse protocol with 135 mM Na_i^+/5 mM Na_o^+, the early increased Na^+ conductance at interpulse intervals of less than 500 ms results in

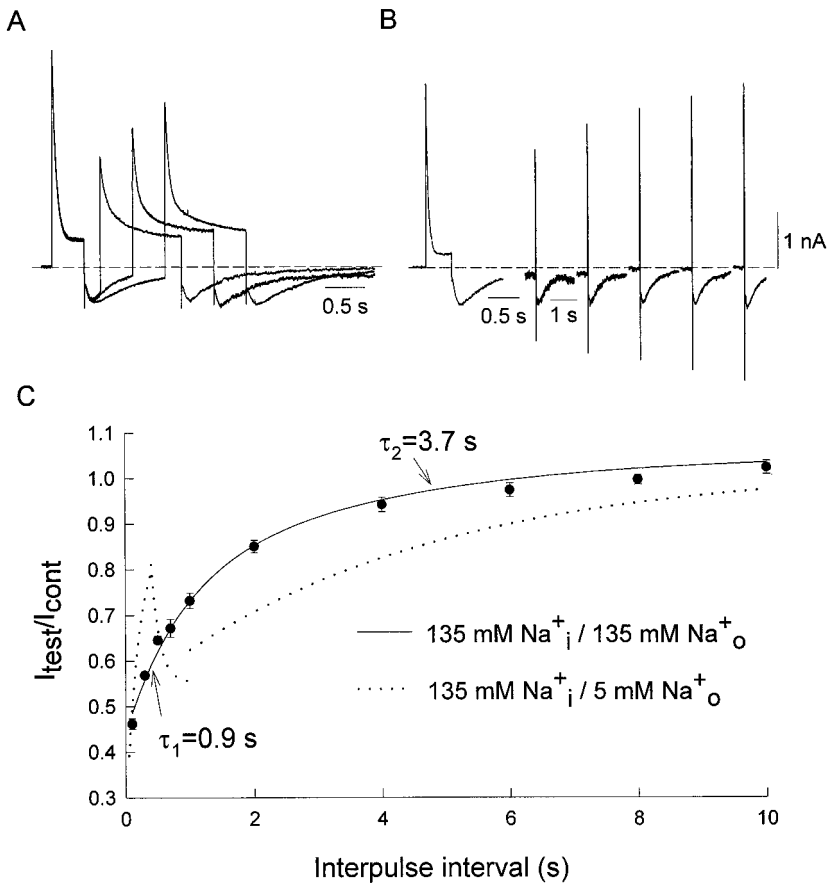

FIGURE 2 Increase in Kv1.5 Na^+ conductance in symmetrical Na^+ during the recovery from C-type inactivation. (*A*) Supernormal currents at short repolarization intervals in 135 mM Na_i^+/135 mM Na_o^+. A 400-ms prepulse to +60 mV from −80 mV conditioned the channels. After repolarization for 200 ms at −80 mV, a 1-s test pulse to +60 mV was given. The protocol was repeated every 20 s, with an increment of the interpulse interval of 400 ms each time. (*B*) Data from another cell. As for *A*, except that the interpulse interval was incremented by 2 s each time. (*C*) Time course for the recovery of the outward Na^+ currents. The test pulse peak outward current (I_{test}) was normalized to the corresponding prepulse current amplitude (I_{cont}), and the ratio I_{test}/I_{cont} was plotted as a function of the interpulse interval. The double-exponential fit had time constants of 0.9 ± 0.2 s (τ_1) and 3.7 ± 1.8 s (τ_2) (n = 4–9 cells). The dotted line represents recovery from inactivation in 5 mM Na_o^+ (redrawn from Fig. 3 *D*).

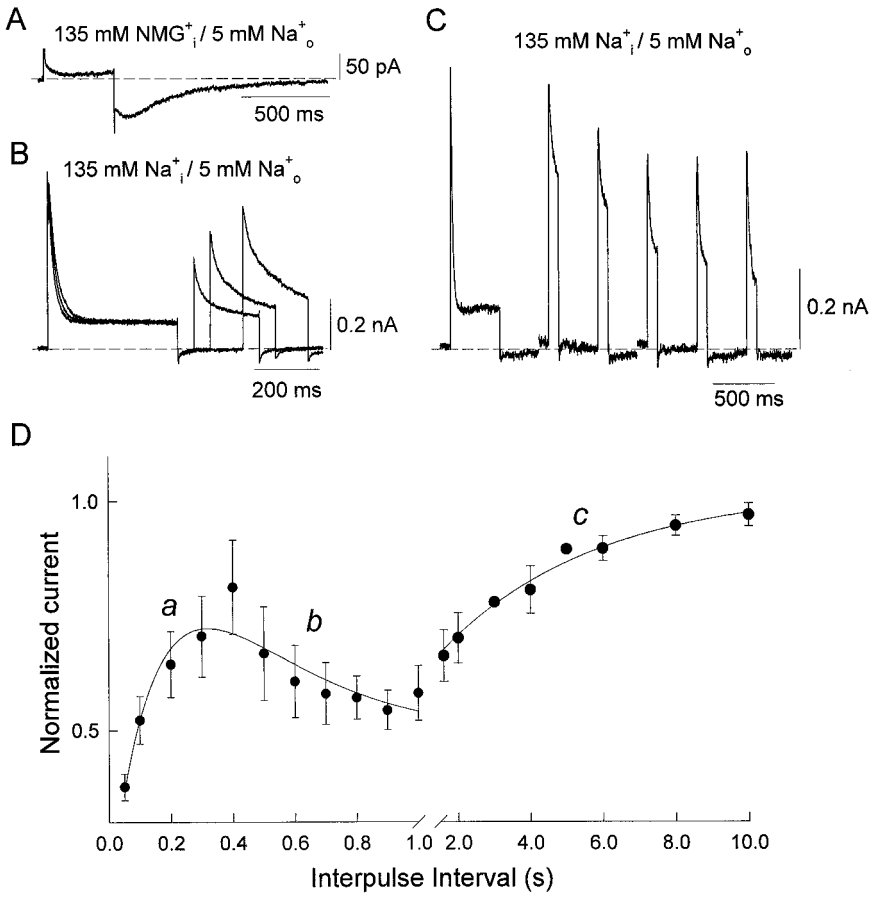

FIGURE 3 Increase of Kv1.5 Na^+ conductance in asymmetrical Na^+ during the recovery from C-type inactivation. (*A*) Appearance of slow inward Na^+ tail current in 135 mM NMG_i^+/5 mM Na_o^+. The pulse was from −80 to +60 mV for 400 ms. (*B*) Supernormal currents at short repolarization intervals in 135 mM Na_i^+/5Na_o^+. A 400-ms prepulse to +60 mV from −80 mV conditioned the channels. After repolarization for 50 ms at −80 mV, a 200-ms test pulse to +60 mV was given. The protocol was repeated every 20 s, and the interpulse interval was incremented by 50 ms each time. (*C*) As for *B*, from another cell, except that the interpulse interval was incremented by 400 ms each time. (*D*) Mean peak test pulse data were normalized to preceding control peak current amplitudes and plotted as a function of the interpulse interval. Note the break in the abscissa after 1 s and the change of time base. Three phases are shown (*a–c*), of which *a* and *b* were fit by a double-exponential function. Phase *c* was fit by a single exponential with a time constant of 4.3 ± 0.9 s ($n = 8$).

outward currents that inactivate slowly (Fig. 3 *B*) and that can be almost equal in amplitude to prepulse currents (Fig. 3 *C*). At interpulse intervals greater than 500 ms the test pulse outward current becomes smaller again, and currents decay more quickly during the pulse, until a minimum is reached at about a 1-s interval (Fig. 3 *C*). At interpulse intervals longer than 1 s a monoexponential recovery of peak current to control levels is seen (Fig. 3 *D*). Mean data in Fig. 3 *D* (note the split time base) show that Na^+ conductance is least immediately after repolarization to −80 mV, but increases rapidly (phase *a*), peaking at ~400 ms after the prepulse, and subsequently declining at intermediate interpulse intervals (phase *b*). At ~1 s, Na^+ conductance reaches a second minimum at ~55% of prepulse peak amplitude and afterward increases again (phase *c*). Phases *a* and *b* correspond to the time course of the tail rising phase and slow decay seen in Fig. 3 *A*. At medium to long repolarization intervals from 1 to 10 s, phase *c* shows a single exponential time course of recovery of peak current ($\tau \approx 4.3 \pm 0.9$ s). This suggests that complete recovery of inactivated channels can take up to 20 s. The data in Figs. 2 and 3 clearly indicate the presence of a high Na^+ conductance state during the recovery from inactivation and the regulation of the recovery time course by Na_o^+.

Inactivation in the recovering channels

Outward currents elicited by a depolarizing step at the time of the peak of the Na^+ inward tail inactivate slowly, and inactivation is voltage dependent, as shown in Fig. 4. Prepulse currents at +60 mV (Fig. 4 *A*) and all positive potentials are rapidly inactivating and can be fit to a single exponential (τ) with almost no voltage dependence (Fig. 4 *B*). Currents induced by test pulses shown in Fig. 4 *A* were better fit by a double exponential (shown as *lines through data points*) with a fast component (τ_1) not significantly different from τ and a slow component (τ_2) that becomes slower at positive voltages (Fig. 4 *B*). Along with the slowing of τ_2 at more positive potentials, a significant increase in the relative amplitude of the slow component of inactivation from 46% to 64% of the total is observed between +10 and +30 mV (Fig. 4 *C*). Using the equation described in Materials and Methods, an estimate of the voltage sensitivity of the inactivating transition (q) was obtained; this was 0.03 ± 0.05 e_0 and 0.05 ± 0.05 e_0 for τ and τ_1, respectively, and 0.11 ± 0.01 e_0 for τ_2. Biexponential inactivation of test pulse currents is very possibly the result of two entry pathways into the inactivated state. The appearance of slowly inactivating currents is not dependent

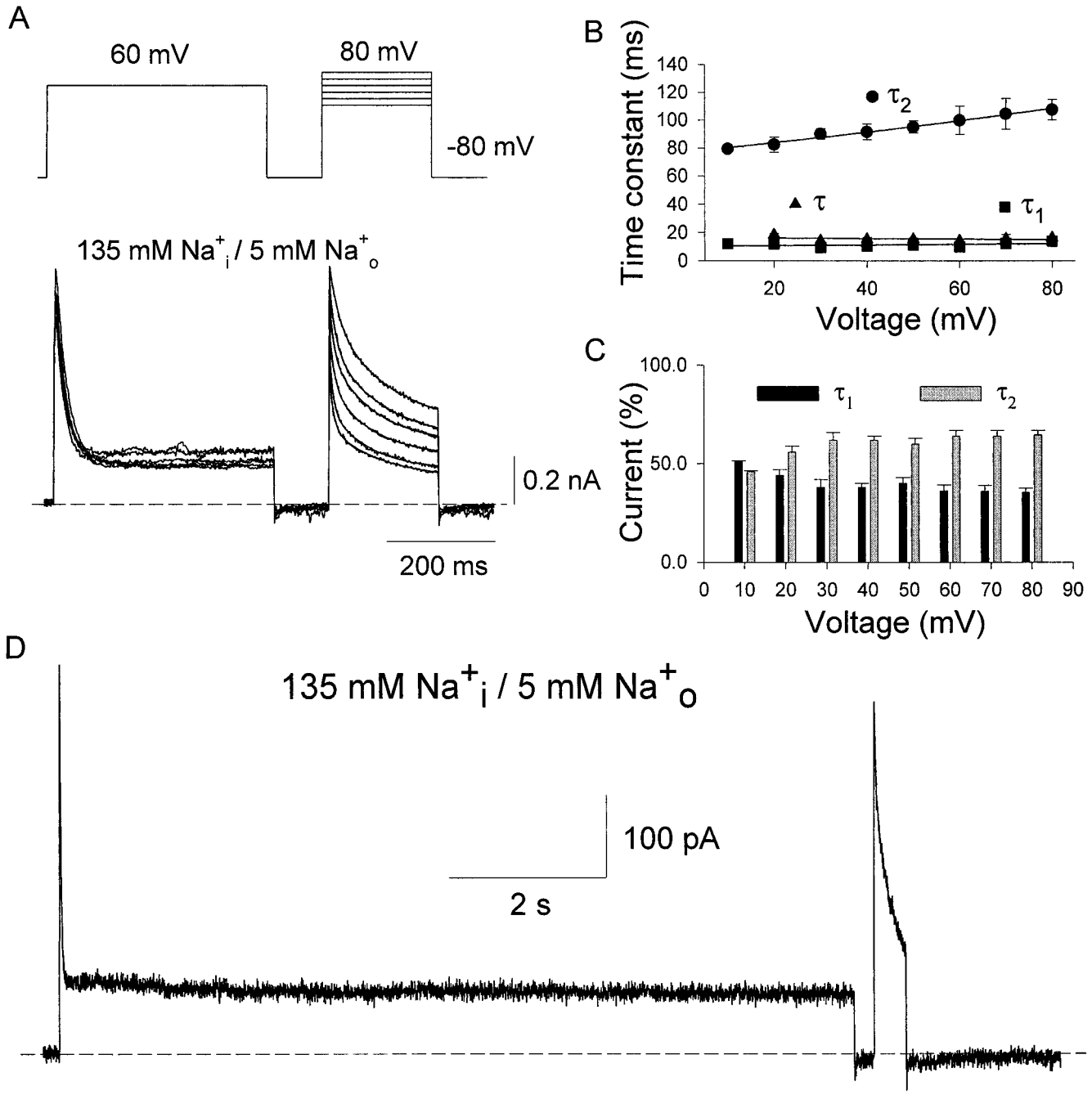

FIGURE 4 Slowed inactivation during the high Na^+-conducting state in Kv1.5 channels. (*A*) 135 mM Na_i^+/5 mM Na_o^+. Currents were recorded every 20 s during 400-ms prepulses from −80 mV to 60 mV, followed by a test pulse to a variable potential between +10 and +80 mV, as indicated in the twin-pulse protocol at top. Lines through test pulse data are biexponential fits to current decay. (*B*) Time constants of Na^+ current inactivation versus depolarization voltage, during the prepulses, fitted to single exponentials (τ), and during test pulses as in *A*, fitted to double exponentials (τ_1 and τ_2). The lines through the data were obtained by fitting τ-*V* curves to obtain *q* (see Materials and Methods). For τ and τ_1, *q* was 0.03 ± 0.05 e_0 ($n = 5$) and 0.05 ± 0.05 e_0 ($n = 9$), respectively, and 0.11 ± 0.01 e_0 for τ_2 ($n = 9$). (*C*) Relative amplitudes of τ_1 and τ_2 from *B* as a function of potential. (*D*) As for *A*, with a 10-s conditioning pulse and 400-ms test pulse, both from −80 mV to 60 mV. The interval between the two pulses was 250 ms.

on the duration of the conditioning depolarization. After a 10-s prepulse to +60 mV, the current induced by a test pulse where the interpulse interval is 250 ms still shows a markedly reduced rate of inactivation (Fig. 4 *D*). These observations support the view that on repolarization the inactivated channels pass through an intermediate state of higher Na^+ conductance than that of the inactivated state. As Na^+ could significantly delay inactivation in this state, it

is very possible that the Na^+ affinity for the intrapore binding site(s) is higher than in the open state (Kiss and Korn, 1998). In the diagram below we have named this highly Na^+-permeable intermediate state R:

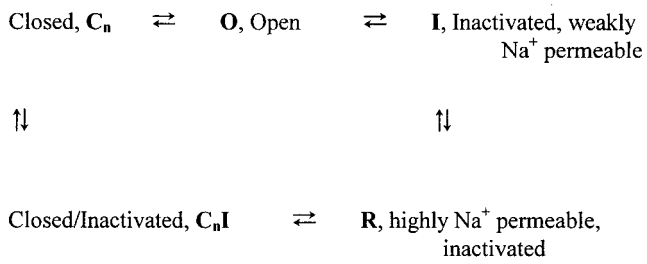

Prior inactivation is obligatory for entering the R state during deactivation

Experiments on the R487V mutant channel of Kv1.5 support the relationship between C-type inactivation and the R state (Fig. 5). R487 is located in the outer vestibule (Aiyar et al., 1995; Doyle et al., 1998) and participates in the external tetraethylammonium-binding site (Kavanaugh et al., 1992; Bretschneider et al., 1999). Replacement of R487 with valine markedly reduces the rate of C-type inactivation of Kv1.5 Na^+ currents, so that during prolonged depolarization only limited inactivation is observed (Fig. 5 *A*). In symmetrical Na^+ solutions, we can also visualize the tail current on deactivation after short and long pulses. This allows us to use this mutant to test whether the slow Na^+ tail appears when inactivation is impeded. We recorded the tails after 100-ms and 14-s depolarizing pulses and observed that the tails show fast kinetics of decay, characteristic of open deactivating channels. There is no indication of the slow rising and decay phase characteristic of Na^+ permeation through inactivated channels (Fig. 5 *B*). The observations on R487V suggest that the slow Na^+ tails in the WT channel are only relevant to the recovery of inactivated channels, and the Na^+-permeant state does not occur within the normal deactivation pathway.

Na^+ permeation through recovering channels is not altered by the conditioning ion species

We suggest that the R state is an intermediate conformation during the recovery from C-type inactivation. It is important to know whether this state is Na^+-dependent; that is, is it only seen when Na^+ permeates the channel, or can the existence of this state be linked to conditions that are present when K^+ permeates the channel? The experiments in Fig. 6 address these issues. Depolarizations to +10 mV with 1 mM K_o^+ in the external solution, in addition to NMG_i^+/NMG_o^+, give a rapidly inactivating inward K^+ current during the pulse, followed on repolarization by an inward tail current with a fast decay kinetics (Fig. 6 *A*). This fast inward tail current reflects K^+ current through open channels during the deactivation. When NMG_o^+ is replaced by Na^+ ions, after the initial fast K^+ tail, a slow tail appears with a rising phase and a slow decay that results from Na^+ flux through deactivating inactivated channels (Fig. 6 *B*). This experiment indicates that the channels in the R state are incapable of conducting K^+ ions, but only allow Na^+ permeation.

The state still seems to be an integral part of the recovery from inactivation pathway when the pore is "conditioned" during the inactivation process by K^+ ions. On depolarization to +60 mV with a K_i^+ concentration of 5 mM and 135 mM Na_o^+, an outward K^+ current was induced with a rapid decay (Fig. 6 *C*). This C-type inactivation is fast when compared to the inactivation rate obtained in 135 mM K_i^+/5

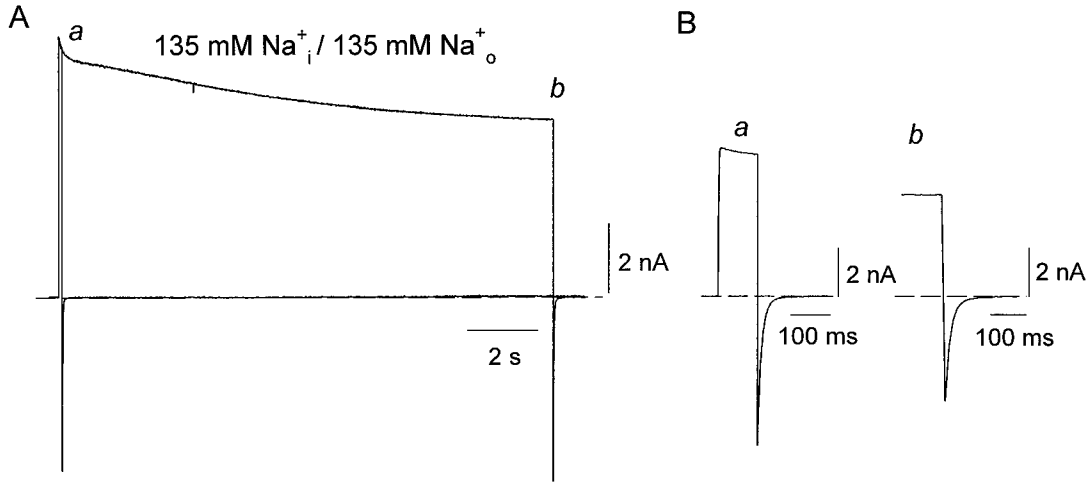

FIGURE 5 Na^+ currents through R487V mutant Kv1.5 channels. (*A*) Whole-cell current recordings from Kv1.5-R487V in 135 mM Na_i^+/135 mM Na_o^+. The depolarizing pulse was from −80 mV holding potential to +80 mV for 100 ms or 14 s. Traces from the same cell are superimposed. (*B*) Expanded scale tail current recordings from the experiment shown in *A*. Trace *a*, 100-ms depolarization; trace *b*, end of 14-s pulse.

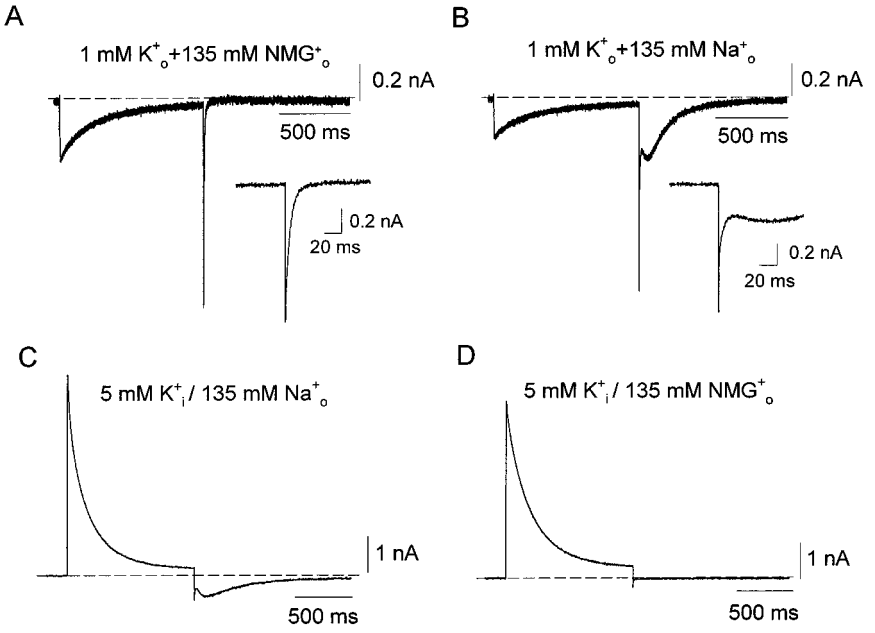

FIGURE 6 Na^+ permeation and K^+ permeation through Kv1.5 channels both allow slow Na^+ tail currents. (*A*) 135 mM NMG_i^+/1 mM K_o^+ + 135 mM NMG_o^+. The current was recorded for 1 s at +10 mV from −80 mV. The inset is the enlarged tail current. (*B*) As for *A*, except that external NMG^+ was replaced by 135 mM Na_o^+. *A* and *B* were obtained from the same cell. (*C*) 5 mM K_i^+ + 135 mM NMG_i^+/135 mM Na_o^+. The pulse was from −80 mV to +60 mV for 1 s. Note the rising phase and the slow decay of Na^+ tail current. (*D*) As for *C*, except that external Na^+ was replaced with 135 mM NMG_o^+. *C* and *D* were recorded from the same cell. Similar results were seen in five other cells.

K_o^+ (Fig. 1 *A*). On repolarization to −80 mV, the same slow Na^+ tail as that seen in the above symmetrical Na^+ experiments appears. Substitution of external Na^+ by NMG^+ prevents this slow Na^+ tail (Fig. 6 *D*) because NMG^+ cannot pass through the channels. The experiments show that when Kv1.5 inactivates while conducting K^+ it undergoes the same recovery process as when the pore was conditioned with Na^+ (Figs. 1–5). Data in Fig. 6, *C* and *D*, support the view that the R state does not result from an abnormal occupation of the pore by Na^+ ions. On the contrary, the state appears to represent a general conformational change of the pore during recovery from C-type inactivation, regardless of the species of permeant ions occupying the pore during the induction of C-type inactivation.

Voltage-dependent recovery of C-type inactivated channels

Our observations suggest that the inactivated channels transit to an R state and then deactivate to closed-inactivated states, which generates the rising and falling phases of the Na^+ tail. In symmetrical 135 mM Na_i^+/Na_o^+, a single voltage pulse reveals a transient outward Na^+ current followed by a sustained outward current that is ~10% of the peak and reflects Na^+ permeating inactivated channels (Fig. 7 *A*). Thus, after a 200-ms depolarization, all of the channels are inactivated. On repolarization, the initial current jump is almost equal to the amplitude of the outward sustained current, representing inward Na^+ current through C-type inactivated channels. Subsequently, although current develops in the inward direction, the peak inward tail is markedly smaller than the peak outward current through the open channels. This suggests that deactivation is significantly faster than the transition to the R state (Fig. 10). However, if the two processes are coupled together, the measured time constant of the decline will be slowed by the rate-limiting transition of channels from inactivated states to the R state, which should also mean that the deactivation is governed by the transition to the R state. This situation recalls the gating of some Na^+ channels (Aldrich et al., 1983), and by analogy, the slow falling phase of the tail does not exclusively imply a slow exit transition from the R state. Data in Fig. 7 *B* show current records where, after a 400-ms pulse to +60 mV, the membrane was repolarized to different voltages from −120 mV to −20 mV. The enlarged tail current recordings show that after an initial step of inward current resulting from a change in driving force, the inward currents increase further and then slowly decay to zero. At more negative repolarization potentials, the rising phase is more apparent, and the decay is also faster, so that the peak inward current occurs at earlier times. The rising and decay phases of these Na^+ tail currents were analyzed by fitting them with double-exponential functions. These fits are shown as the lines through data in the inset panel to Fig. 7 *B*. In Fig. 7 *C*, the rising and decay phase time constants, τ_1 and τ_2, respectively, are plotted against repolarization voltages. The slope gives a 10-fold change in time constant over ~113 mV for τ_1 and 117 mV for τ_2, respectively, which suggests that both are driven by a single voltage-sensitive process, i.e., that transition to the R state governs deactivation to closed inactivated states.

At −20 mV in Fig. 7 *B*, almost no Na^+ tail was apparent on repolarization. This suggested that at this potential the transition from the inactivated state to the R state either was prevented or was extremely slow. We also questioned

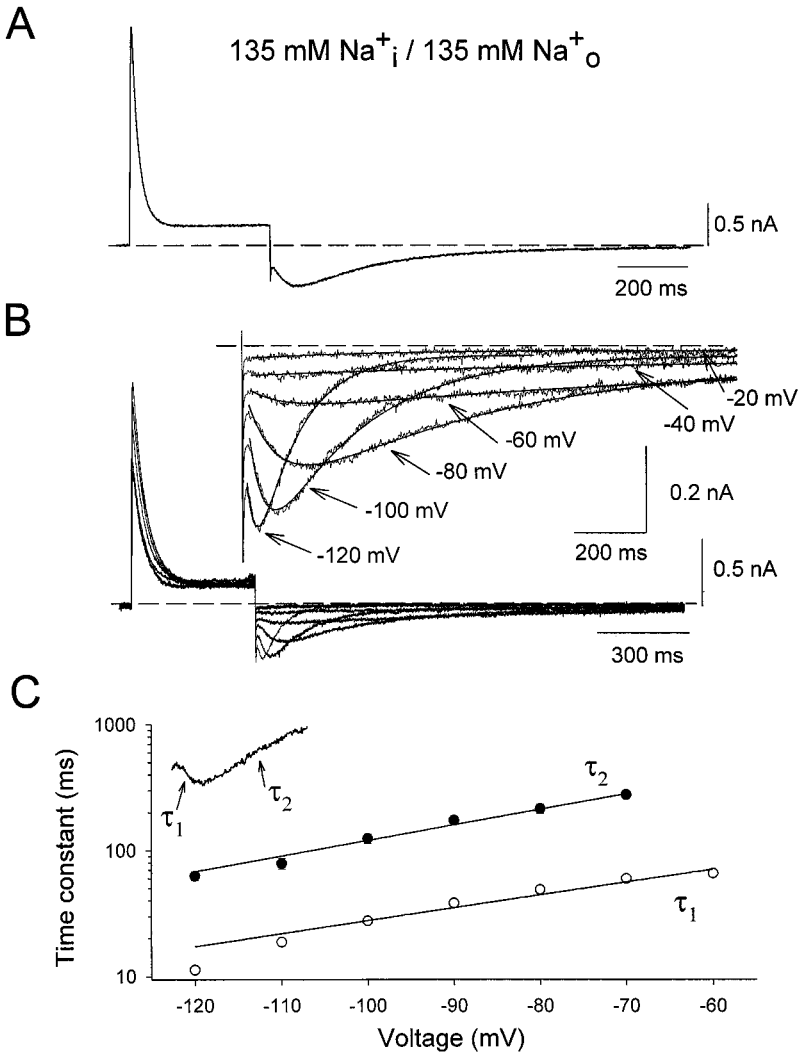

FIGURE 7 Voltage-dependent deactivation of inactivated Kv1.5 Na^+ currents. (*A*) Symmetrical 135 mM Na_i^+/Na_o^+. The current was recorded at +60 mV for 400 ms from −80 mV. (*B*) As for *A*, except for repolarization to different voltages between −120 and −20 mV. The pulse was given every 20 s. Current tracings are shown at 20-mV repolarization intervals. (*B, inset*) Enlarged tail currents. Biexponential fits to obtain τ_1 and τ_2 are shown as lines through data points. The fast initial current spike is caused by capacitance. (*C*) Time constants of Na^+ current deactivation versus repolarization potential. τ_1 was fitted to the rising phase of the tail current, while τ_2 was fitted to the slower decay phase, as indicated in the inset.

whether, as a result, channels could recover from inactivation if they did not transit into the R state. We tested this idea by using symmetrical 135 mM Na_i^+/Na_o^+ to examine recovery from inactivation at −20 mV and to visualize Na^+ tail currents (Fig. 8). After a 400-ms prepulse to +60 mV, the potential was held at −20 mV for 10 s. During this time, no slow Na^+ tail current was observed. A subsequent test pulse to +60 mV induced a test current showing little recovery from inactivation (Fig. 8 *A*). If a 2-s period at −80 mV was applied just before the test pulse (Fig. 8 *B*), the slow Na^+ tail was observed, and the peak outward current during the test pulse was 79% of that for the prepulse. Averaged data are shown in Fig. 8 *C*. A 10-s period at −20 mV resulted in a test pulse peak current that was only 15.7 ± 1.2% (n = 7) of the peak occurring during the prepulse. However, a 2-s period at −80 mV just before the pulse increased the peak test pulse current amplitude to 77.6 ± 1.1% (n = 8) of the prepulse current. This indicates that almost no channels progressed to the R state during the 8-s period at −20 mV. Almost no channels recovered from inactivation during the 10-s interval when held at −20 mV, suggesting that the R state is a required step in this pathway to recovery from inactivation.

Time course of recovery from inactivation measured by fast tail reactivation

In symmetrical Na^+, when the peak outward current recovery from inactivation was measured it was biexponential (Fig. 2), and it was even more complex in asymmetrical 135 mM Na_i^+/5 mM Na_o^+ (Fig. 3). The time course of peak current reactivation reflects contributions from channels in the R state, as well as channels that eventually return to closed states and open normally to O (upper pathway in the model shown in the text). A way to separately evaluate the second group of channels, available in normal closed states, is to examine the reactivation of fast tail currents on repo-

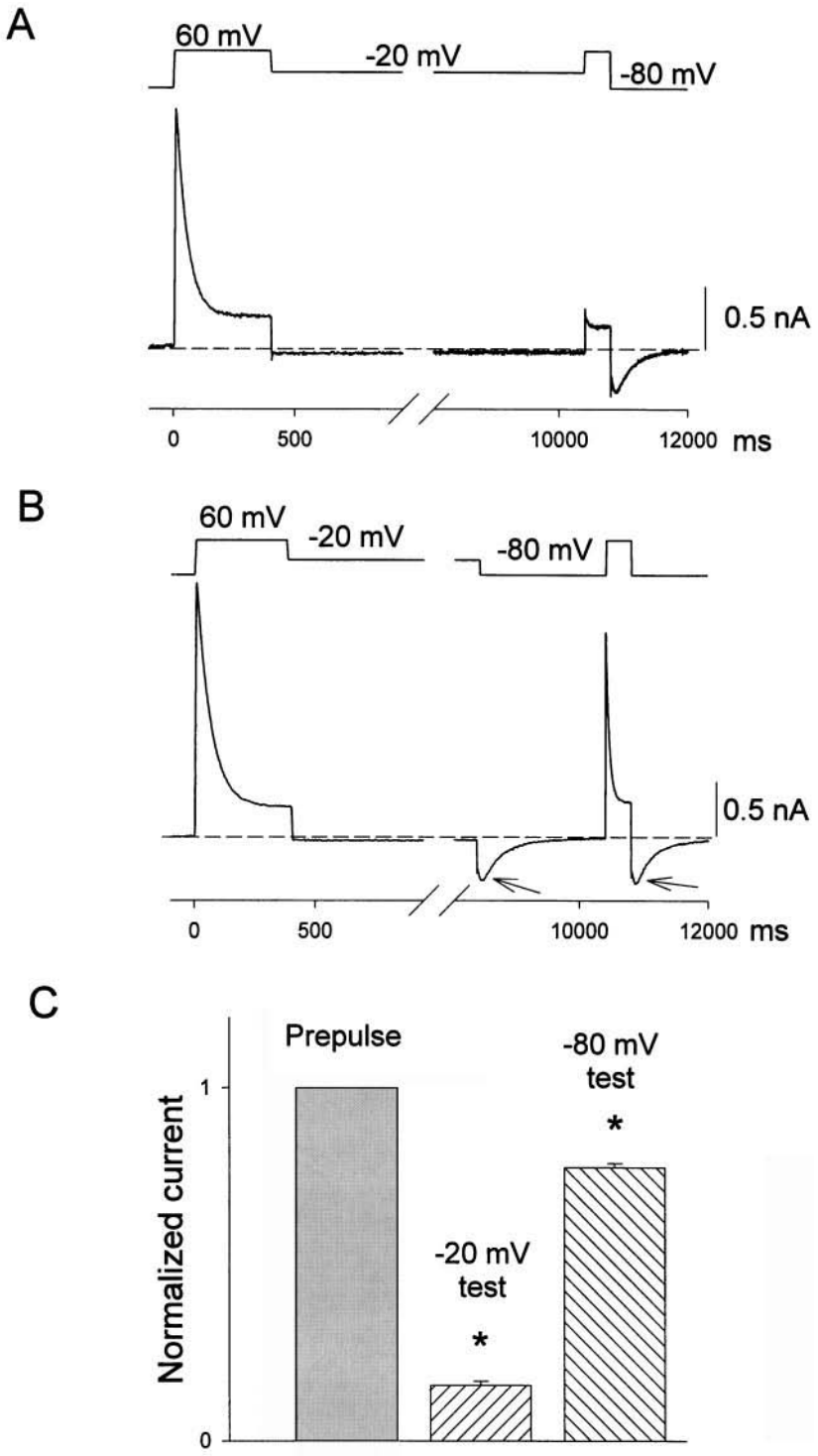

FIGURE 8 Repolarization negative to −20 mV is required to allow recovery of C-type inactivated Na^+ currents. (*A*) In symmetrical 135 mM Na_i^+/Na_o^+, current was recorded during a control prepulse to +60 mV and, during a second test pulse to +60 mV, after 10 s at −20 mV. (*B*) As for *A*, with an additional 2-s repolarization to −80 mV before the second depolarizing test pulse, as indicated in the pulse protocol shown above the current recording. Arrows indicate Na^+ tail currents at −80 mV. Note the breaks in and change of time base in both *A* and *B*. (*C*) Peak outward currents during the test pulses normalized to the currents in preceding prepulses. Hatched bar data were obtained from eight cells, using the protocol in *A* (−20 mV test) and *B* (−80 mV test). * Significant difference from prepulse amplitude, $p < 0.05$.

larization. This tests the number of channels able to deactivate rapidly from open to closed states and thus serves as an index of channels capable of opening.

The experiment was performed in symmetrical 135 mM Na^+ solutions (Fig. 9). A prepulse to +80 mV from −80 mV for 400 ms drove all of the channels to the inactivated state, and after various interpulse intervals a test pulse for 20 ms was applied. As shown earlier in Fig. 1 *C*, a 20-ms depolarization activates channels but is too short to allow significant inactivation to occur. This means that the amplitude of rapidly decaying tails on repolarization is an index of the number of available channels deactivating normally at the negative voltages. In Fig. 9 *A*, at the end of the prepulse, tails show a rising phase and slow falling

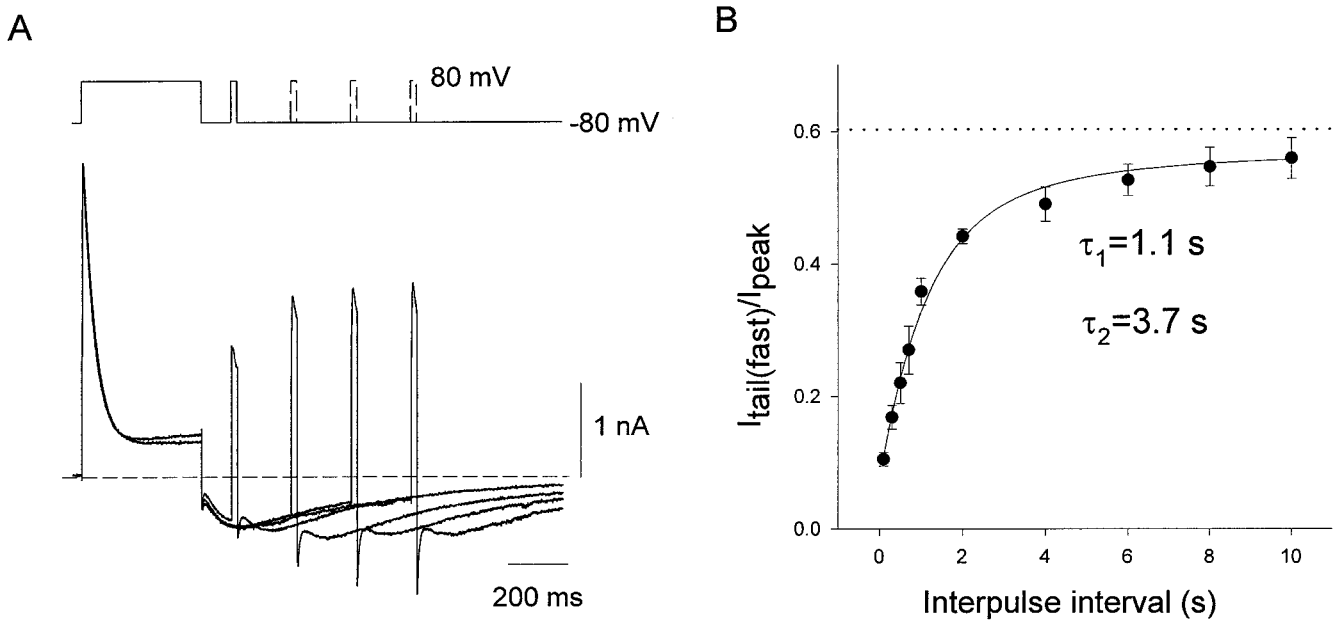

FIGURE 9 Recovery of C-type inactivated Kv1.5 channels in symmetrical Na^+ solutions. (*A*) Symmetrical 135 mM Na_i^+/Na_o^+. Currents were recorded using the twin-pulse protocol shown at the top, which was repeated every 20 s to allow full recovery from inactivation between tests. A 400-ms prepulse was followed by a 20-ms test pulse after a variable interpulse interval. (B) Time course for the recovery of the fast Na^+ tail current ($I_{tail\ (fast)}$). The amplitude was measured from the instantaneous peak to the end of the fast tail and normalized to the peak outward current (I_{peak}) during the prepulse. The ratio was plotted against the interpulse interval. The best fit to data was a double exponential with time constants as 1.1 ± 0.2 s (τ_1) and 3.7 ± 1.3 s (τ_2). The data were obtained from four to nine cells. The dotted line represents recovery to control level, measured as the fraction of fast tail amplitude after a 20-ms depolarization to peak outward current during the prepulse.

phase without any clear fast tail, which implies that at the end of the prepulse all channels have been inactivated. On repolarization the inactivated channels only progress to the R state, as shown by the slow Na^+ tail current. However, with longer reactivation times, a fast tail appears at the end of the test pulses and becomes larger with longer interpulse intervals. For longer reactivation periods data were obtained from experiments as shown in Fig. 2 *B*. The time course of the increase of the fast tail is biexponential with time constants of 1.1 and 3.7 s (Fig. 9 *B*) and reflects the return to normal closed states of the inactivated channels. This agrees closely with the time course of recovery of peak current described in Fig. 2 *C*, and so these data support our hypothesis that the inactivated channels return through the R state and then through closed inactivated states to closed states to fully recover from C-type inactivation.

Another important observation from the data in Fig. 9 *A* is that after intermediate repolarization periods, the amplitude of the slow tail on repolarization after the test pulse is significantly bigger than that just before the test pulse. This suggests that during the depolarizing test pulse, channels in closed inactivated states can be driven rapidly back to the R state, where they become available to conduct Na^+ with a high conductance. This supports the idea put forward in Fig. 7 of rapid reversible deactivation from the R state to closed inactivated states. Together, the observations have informed a more complete model of the experiments described here. This is shown in Fig. 10; this and other models are discussed in the following section.

DISCUSSION

A model of the inactivation and recovery from inactivation of Kv1.5

The diagram in Fig. 10 fills out the state model suggested earlier in the text and was used to simulate inactivation and its recovery in Kv1.5 channels when they are conducting Na^+ ions. The early closed-closed transitions were obtained from our constrained gating current model published earlier (Hesketh and Fedida, 1999). We have included a single open state (O) and a single, absorbing inactivated state (I) occupied on depolarization. On repolarization negative to −20 mV, after a delay, inactivated Kv1.5 channels enter a state with higher Na^+ conductance that we have called R. Channels then rapidly deactivate to closed inactivated states (C_nI) and finally slowly return to closed states (C_n) with a rate γ. We will show that modulation of the C_4I to C_4 transition rate, γ', by Na_o^+ is sufficient to simulate the recovery time course measured experimentally.

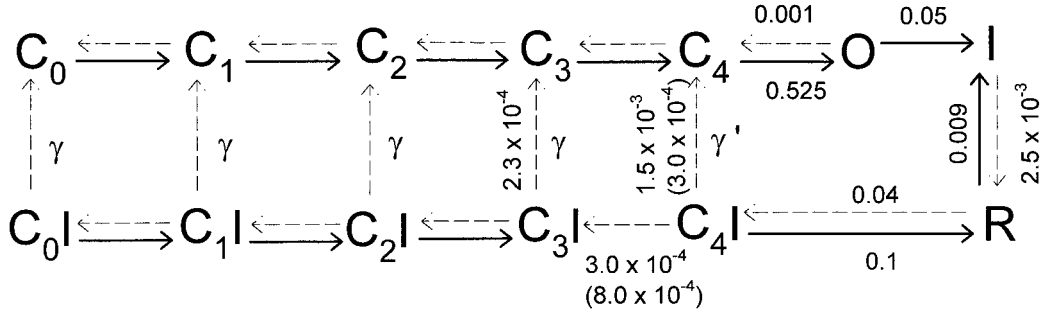

FIGURE 10 State diagram of the model used to describe sodium permeation through Kv1.5. Solid and dashed arrows denote, respectively, dominant transitions at positive (+80 mV) and negative (−80 mV) potentials. Numbers are rate constants for respective transitions in ms^{-1}. For nondominant transitions at either +80 or −80 mV, rates were set to zero. The rates adjacent to each rate were those used in the model simulations of ionic currents under conditions of symmetrical Na^+ (135 mM $Na^+_{i/o}$). Values in parentheses denote changes required to simulate currents under conditions of low external Na^+_o (5 mM). All other rates were obtained from Hesketh and Fedida (1999). The C, I, and R states in the model conduct Na^+ with ratios of 1:0.15:1, respectively. All closed states are nonconducting.

Rapid inactivation of Na^+ currents out of the open state

In Kv channels, C-type inactivation is slowed by the binding of permeant ions to intrapore site(s), such as the selectivity filter (Kiss and Korn, 1998). Intrinsic Kv channel inactivation is almost too fast to observe, but the presence of ions bound at sites within or close to the permeation pathway can delay or prevent this process (Lopez-Barneo et al., 1993; Starkus et al., 1997). K^+ ions have a high affinity for these sites and therefore have a longer dwell time at these sites, so K^+ currents show slow inactivation (Fig. 1 *A*). Normally, open Kv1.5 channels are highly selective for K^+ over Na^+, suggesting that like other Kv channels (Starkus et al., 1997; Ogielska and Aldrich, 1998), Na^+ ions have low affinity for the intrapore sites and a shorter dwell time (than K^+) at these sites. Therefore, C-type inactivation of Kv1.5, like other Kv channels, is facilitated when Na^+ is the permeant cation (Starkus et al., 1998; Kiss et al., 1998; Fedida et al., 1999).

It has been suggested that C-type inactivating channels proceed through three states. Initially channels open from closed states, the open state being highly selective for K^+, but in some channels like Kv1.5, if K^+ is omitted, significant Na^+ conductance can be observed (Fig. 1). In our system, as described in Materials and Methods, we have been able to lower $K^+_{i/o}$ sufficiently to observe clear Na^+ currents through open Kv1.5 channels. Open channels inactivate to a state in which they are partially Na^+ permeant and then proceed to a more distal state from the open state in which ions do not permeate (Loots and Isacoff, 1998; Kiss et al., 1999). It seems that different Kv channels must have different Na^+ permeabilities of this distal state, with *Shaker* channels having a relatively high conductance (Starkus et al., 1997) and Kv2.1 having a much lower conductance (Kiss et al., 1999). Inactivating Kv1.5 channels conducting Na^+ do not appear to go through an intermediate high Na^+ conductance state during depolarization. In symmetrical Na^+_i/Na^+_o the time course of decay of inward tail currents versus the time when currents are interrupted during the onset of inactivation is monoexponential (Fig. 1 *D*). An intermediate state may be present (see below) but is not functionally important in Na^+-conducting Kv1.5 channels. We have found that the process of inactivation in Na^+-conducting Kv1.5 channels can be effectively modeled without including such a state in the simulation (Figs. 10 and 11 *A*).

Inactivation was modeled from data as in Fig. 1 *B*, and the transition from O to I was assigned a rate of 0.05 ms^{-1}. This limited the size of the peak current to 87% of the maximum current expected without inactivation. The experimental data showed that even after a relatively short depolarization, rapid tails on repolarization disappeared (Fig. 1 *C*) and were replaced by slow tails, indicating that inactivation is complete for Na^+ currents through Kv1.5. Results from this protocol were effectively modeled as shown in Fig. 11 *A*. The permeation of sodium through the inactivated state was set at 13% of the conductance through the open state and was obtained directly from the sustained component of outward current during prolonged depolarization (see Fig. 1 text). This gives the rapidly inactivating test pulse current with a sustained level seen in Fig. 11, *A* and *B*. The steady current level is somewhat less than that of *Sh*Δ channels, where the steady-state conductance to Na^+ appears to be ~50% of the open state (Starkus et al., 1997). Thus, although the inactivated state is Na^+ permeable, its conductance is much less than that of the open state. On repolarization after brief depolarizations, open channels deactivate rapidly from O to C_4 to give the fast tail component, and inactivated channels in I progress to R to give the rising phase of the slow Na^+ tail current, as clearly observed in Fig. 11 *A*. As the length of the prepulse is increased, fewer channels are available to deactivate from O, so the fast tail amplitude declines and the slow tail increases (Fig. 11 *A*).

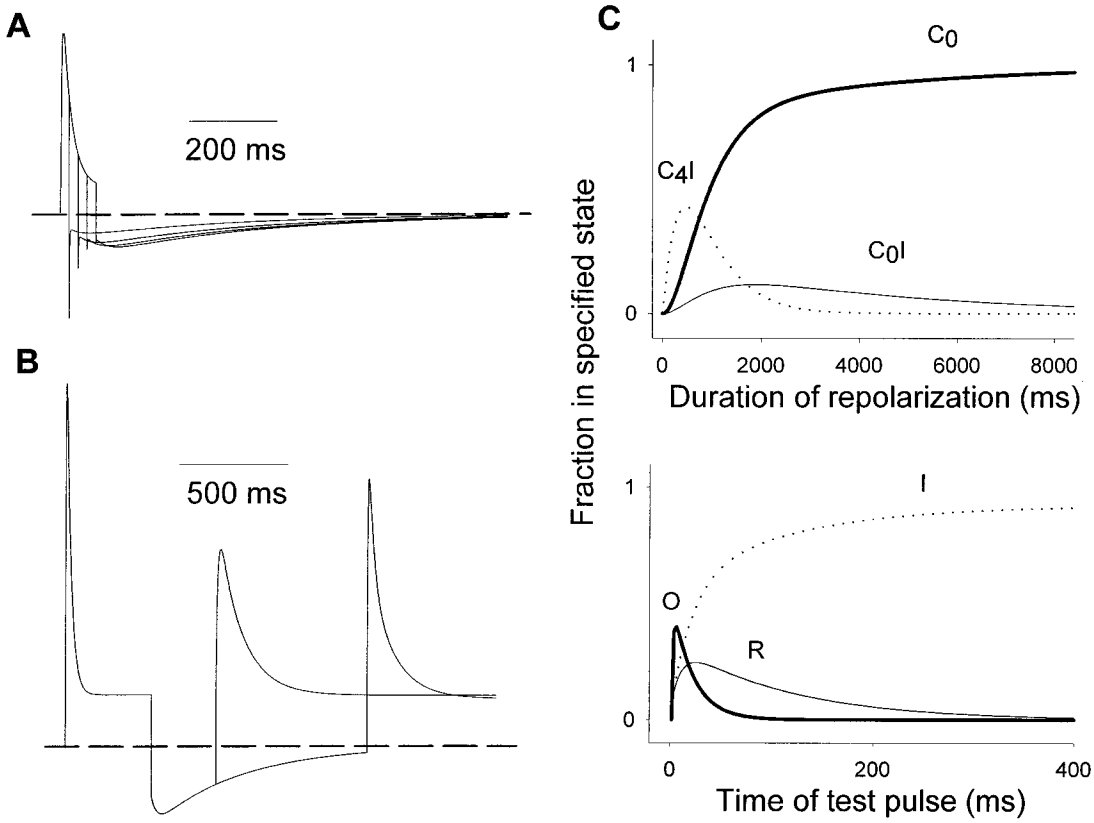

FIGURE 11 Simulations of Kv1.5 Na^+ current inactivation produced by the model in Fig. 10. (*A*) Simulation of current inactivation and tails during brief depolarizations in symmetrical 135 mM Na_i^+/Na_o^+. An initial 20-ms depolarization was given from −80 to +80 mV, and this was incremented by 20 ms for each subsequent pulse. With increasing test pulse duration, the initial fast tail was progressively reduced, as the rising phase became apparent. (*B*) Model simulation of ionic current in the presence of symmetrical sodium (135 mM $Na^+_{i/o}$). The simulation protocol involves an initial 400-ms depolarization to +80 mV followed by a repolarization to −80 mV, 300 ms or 1 s in length. Repolarization is then followed by a test pulse to +80 mV lasting 1 s. The dashed line denotes zero ionic current. (*C*) Changes in the proportion of channels in specific states during various phases of the simulation protocol illustrated in *B*. (*Top*) Proportion of channels in state C_0 (*thick line*), C_4I (*dotted line*), and C_0I (*thin line*) during the repolarization pulse. (*Bottom*) Proportion of channels in state I (*dotted line*), R (*thin line*), and O (*thick line*) during the second test pulse in *B*, after a 1-s repolarization period.

A high Na^+ conductance state on repolarization

After any initial fast tail decay there is a slow increase in the peak of the inward Na^+ tail current in both symmetrical (Figs. 1 *C* and 2 *A*) and asymmetrical (Fig. 3 *A*) Na^+. The rising phase of slow tail currents is more prominent than that in *Sh*Δ, which was only observed at very negative potentials, below −110 mV. To indicate in the model (Fig. 10) that this Na^+-conducting state is an intermediate state during the recovery from inactivation and kinetically distinct from the normal open pore conformation, we have designated by R the highly Na^+-permeable state. This state is in the pathway of normal recovery from inactivation, as this tail cannot be observed (Fig. 7), and recovery from C-type inactivation is prevented (Fig. 8), unless the tail is allowed to develop on repolarization negative to −20 mV. The state is a direct consequence of inactivation, and the R487V mutant that does not inactivate in Na_i^+/Na_o^+ does not show slow Na^+ tail currents (Fig. 5). For a convenient model simulation, we assumed that the Na^+ conductance of the channels in the R state is the same as that in the open state. Alternative models in which the small tail current size (relative to outward current amplitude) was the result of a low conductance of the R state failed to give large enough outward currents during test pulses to simulate experimental observations (e.g., Figs. 2–4).

Upon repolarization, the transition to the R state produces a slow tail current with a marked rising phase due to the modeled conductance ratio of 0.13 of I versus R (Fig. 11 *B*). The small size of the tail relative to the current during the prepulse (see also Fig. 2) suggests that channels are rapidly taken out of the R state through deactivation to the C_4I state. In Fig. 7 we noted the interdependence of these two transitions, so that the rates cannot be constrained from the data. However, a reasonable prediction of the tail current time course can be obtained with assigned rates of 0.0025 ms^{-1} for the I to R transition and 0.04 ms^{-1} for the R to C_4I transition. The 16-fold faster deactivation rate predicts an appropriately small peak tail combined with a good predic-

tion of the tail decay time course (Fig. 11 *B*). The tail current decays to the baseline in ~1 s, suggesting that channels are completely removed from both the R and I states during this time period. Model predictions of the proportion of channels in the different closed states along the deactivation pathway during the period of repolarization are shown in Fig. 11 *C* (*top*).

A second important difference between the slow Na^+ tail in Kv1.5 and that in *Sh*Δ is that Na^+ and Li^+ tail permeation was blocked by 5 mM K_i^+ in *Shaker*. In Kv1.5 the Na^+ tail on deactivation was not qualitatively affected by 5 mM K_i^+ in the pipette and the consequent outward K^+ current on depolarization (Fig. 6). This result suggests that even when the channel is K^+-conducting during the onset of inactivation, as long as there is not enough K^+ to inhibit Na^+ influx, Na^+ can enter as slow tail currents during the process of recovery from inactivation.

Slow deactivation and decay of the Na^+ tail currents

At the negative repolarizing voltages, Na^+ tail currents decay to zero in ~1 s. Because the duration of the slow Na^+ tail (~1 s) is about one order of magnitude less than the time required for full recovery from inactivation (~ 20 s), we presume that these channels deactivate from the R state to closed inactivated states (C_nI) as suggested for *Sh*Δ channels (Starkus et al., 1997). We assume that the inactivated channels have to progress through the R state and the closed inactivated states to complete the recovery process to closed (C_n) states (Fig. 10). The relative rate constants for recovery from I through O to C_4 are too low to permit recovery from inactivation by this route and are set to zero in the model. At negative potentials, the R to C_4I transition is essentially irreversible, as suggested experimentally by the tail that decays fully to the baseline (Fig. 7). From the C_4I state, the channel may then either recover quickly with the rate γ' or proceed further along the deactivation pathway through an irreversible transition to C_3I. The channel will then quickly deactivate along these earlier closed inactivated states, and at any point along the deactivation path, the channel can recover to the parallel closed noninactivated states, but with a rate γ that is slower than γ'.

Modeling of test pulse currents

In both symmetrical and more obviously in asymmetrical Na^+, application of a test pulse to +80 mV soon after a prepulse results in currents that appear to have a rapid availability and that reinactivate with a markedly reduced biexponential rate (Figs. 2–4). These observations support the idea that the state occupied by inactivated Kv1.5 channels at negative potentials (and subsequently when depolarized in this state) is different from the normal open state. These supernormal currents can be accounted for by channels rapidly reentering the R state from the C_4I state. This predicts the amplitude of test pulse currents seen after even very short repolarizations, which are much larger than can be accounted for by the slow recovery from inactivation (Fig. 11 *B*). As observed experimentally (Figs. 2–4), these supernormal currents decay more slowly than the prepulse current, and this is presumed to be due to a low R to I transition rate, which was set to 0.009 ms^{-1}. This value was obtained from the observed time constant of this slow decay of 110 ms (Fig. 4 *B*). This transition is also absorbing at positive potentials, inasmuch as the steady-state level of the test pulse current is approximately the same as the steady-state current during the prepulse (Figs. 2 and 3). Therefore, in both cases, 100% of the channels are in the inactivated state at the end of the pulses (Fig. 11, *B*, and C, *bottom*). It was noted that for the shortest intervals, the inactivation rates of test pulse currents were slowest (Figs. 2 and 3). This is accounted for by most of the current coming from closed inactivated channels reentering the R state, with its slow progression to I (Fig. 11 *B*). This transition also accounts for the very large slow tails after the very brief test pulses in Fig. 9 *A*. Channels are driven from C_4I to R by the 20-ms depolarization, and these channels conduct on repolarization to give larger tails.

As channels begin to slowly recover from inactivation, to the upper set of transitions in Fig. 10, a fast decay component develops within the test pulse currents. This represents channels opening normally and inactivating from the open state at a rate of 0.05 ms^{-1} (see above). This was clearly seen experimentally (Figs. 3 and 4) and gave the test pulse currents a double exponential time course due to the simultaneous presence of the slower transition from R to I. The fast decay amplitude increases relative to the slow decay amplitude with longer repolarizing pulses, as more channels are able to decay from the open state when they have completed the recovery from inactivation (compare Figs. 2 *A* and 11 *B*). An illustration of the channel states during the second test pulse current in Fig. 11 *B* after a 1-s period of repolarization is shown in Fig. 11 *C* (*bottom*). There is a mixture of channels in O and R at the start of the pulse, and both transit independently into the absorbing inactivated state, I, but at different rates. After short test pulses, the presence of a fast tail provides an index of the number of channels in the open state relative to the number in the R state. Experimentally we found that this fast tail development has a double-exponential time course, suggesting an opportunity for channels to recover either slowly or quickly (Fig. 9 *B*). The faster recovery is represented by the γ' transition, which is assigned a rate of 0.0015 ms^{-1} (τ = 667 ms) in the model and is much faster than the 0.000235 ms^{-1} slow recovery rate, γ. The latter was obtained directly from the time course of slow recovery of either the peak outward current (Figs. 2 and 3) or the slow phase of tail reactivation (τ = 3.7 s in Fig. 9).

Na_o^+ modulation of the C_4I to C_4 transition rate

The fast component of recovery from inactivation, indexed by the recovery of outward currents (Fig. 2) and the reappearance of the fast tail current (Fig. 9) in symmetrical 135 mM $Na_{i/o}^+$, has an amplitude threefold greater than the amplitude of the slow component. This was used as a guide to determine the relative rates of γ' versus the irreversible C_4I to C_3I transition, which was assigned a rate of 0.0003 ms^{-1}. This allowed simulation of the recovery of test pulse current amplitudes in symmetrical 135 mM Na^+ as shown in Fig. 12 *A* (compare with Fig. 2). Time constants of 0.9 and 3.7 s measured experimentally (Fig. 2) fitted the recovery time course of modeled currents (Fig. 12 *B*). The model also illustrates the accelerating inactivation rate of test pulse currents after longer repolarization times, caused by increasing numbers of channels reaching closed states along the upper pathway (Fig. 10), which are available to open and then inactivate rapidly from the open state. An example is also given in the inset of Fig. 12 *A* of a brief test pulse current like those given experimentally in Fig. 9 *A*, to illustrate modeling of the two components of the tail. The simulated test pulse applied after an 8-s repolarization period gives a brief outward current, followed by a fast tail component that reflects channels deactivating from open states to normal closed states. This is followed by a slow Na^+ tail that reflects channels left in C_4I reentering the R state and conducting Na^+ before they deactivate again to closed inactivated states (C_4I).

The multiple phases of test pulse current reactivation in low Na_o^+ were simply modeled by slowing the rate of fast

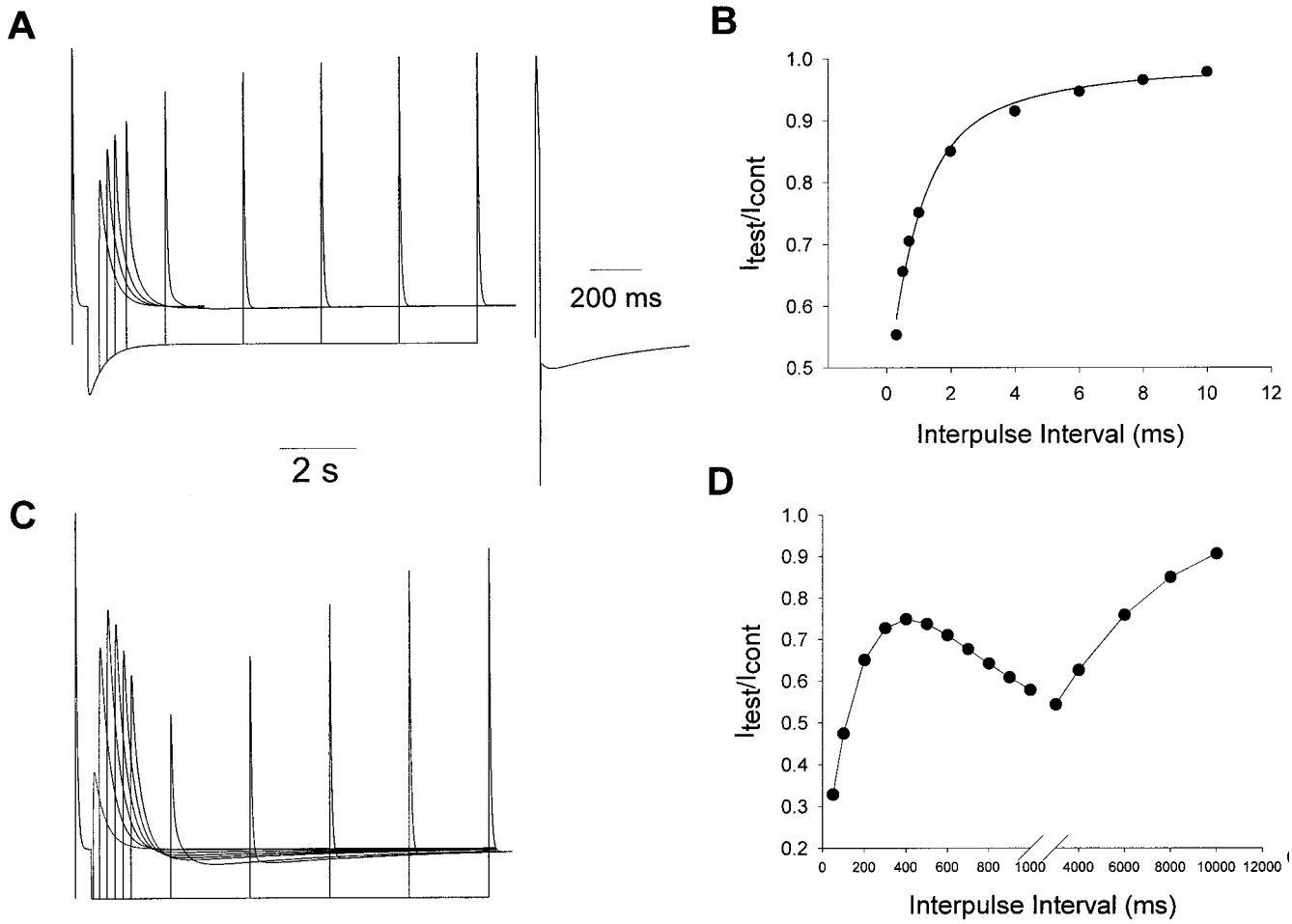

FIGURE 12 Model simulations of Na^+ ionic currents and recovery from inactivation. (*A*) Model simulation of ionic current recovery after an inactivating test pulse (+80 mV, 400 ms), in the presence of symmetrical 135 mM $Na_{i/o}^+$. Repolarization times were 300 ms, 500 ms, 700 ms, 1 s, 2 s, 4 s, 6 s, 8 s, and 10 s, and test pulse durations were 0.3–2 s. The inset shows a single ionic current trace during a 20-ms depolarization, after an 8-s repolarization period. (*B*) Peak level of test pulse outward current relative to peak level of prepulse current as a function of the length of the repolarizing pulses. Points were obtained from the simulations illustrated in Fig. 11 *A*. The smooth line through the points represents a double-exponential curve with time constants of 0.9 and 3.7 s that were obtained from the experimental data illustrated in Fig. 2 *C*. (*C*) Model simulation of ionic currents with a protocol identical to that in *A*, but in the presence of 5 mM Na_o^+. (*D*) Peak level of test pulse current relative to peak level of prepulse current as a function of the length of the repolarizing pulses. Points were obtained from the simulations illustrated in Fig. 11 *C*. Lines through points do not represent any function.

recovery (γ') by fivefold (Figs. 10 and 12, *C* and *D*). This produced qualitative agreement with the experimentally obtained test pulse currents (Fig. 3), which increased with very short repolarizations and then decreased in amplitude at intermediate intervals, followed by a slow increase corresponding to the classical slow recovery from inactivation. To achieve a more accurate simulation, the commitment step was sped up slightly to remove channels more quickly from the C_4I state to the C_3I state. This rate was changed from 0.0003 ms^{-1} to 0.0008 ms^{-1}, a 2.7-fold change (Fig. 10). Therefore, by changing only two rates, the model can simultaneously account for the test pulse amplitudes in both ionic conditions. The data and model then suggest a Na^+-dependent modulation of recovery from inactivation at early steps in the deactivation pathway.

Multiple inactivation states within the inactivation pathway

The data on Na^+ current inactivation and the monotonic correlation of outward current decay with the decay of fast inward tail currents obtained in symmetrical 135 mM Na_i^+/Na_o^+ solutions did not give any suggestion of the presence of more than one inactivated state at depolarized potentials (Fig. 1, *C* and *D*). In the experiments of Kiss et al. (1999) small concentrations of K_i^+ were used to demonstrate changes in inward tail currents during the onset of C-type inactivation. We have reproduced this experiment in Kv1.5; representative data are shown in Fig. 13. Here inclusion of 5 mM K_i^+ with 135 mM NMG_i^+ slowed the onset of C-type inactivation significantly. For very short depolarizations, small inward Na^+ tails are seen. For longer depolarizations, tails become larger and then smaller again. The recovery from inactivation was so slow in this experiment (cf. Figs. 2 and 3) that some cumulative inactivation is present, especially after longer depolarizing pulses. Still, as demonstrated by Kiss et al. (1999), the peak inward Na^+ tail increases and then decreases again. This points to the occupancy of an extra state in the pathway on the way to a relatively lower Na^+ conductance distal inactivated state. The tail current changes are not caused by changes in K_i^+ and K_o^+ through accumulation and depletion, as omission of Na_o^+ prevents the observance of any tail currents at all (Fig. 13 *B*). If we extend our model to include an intermediate higher Na^+ conductance state in the inactivation pathway, I_1, and our absorbing state is now I_2 (Fig. 13 *C*), the model can adequately predict many features of the tail current behavior as shown (Fig. 13 *D*). It is interesting that the tail currents now have a morphology, in experiments and in the

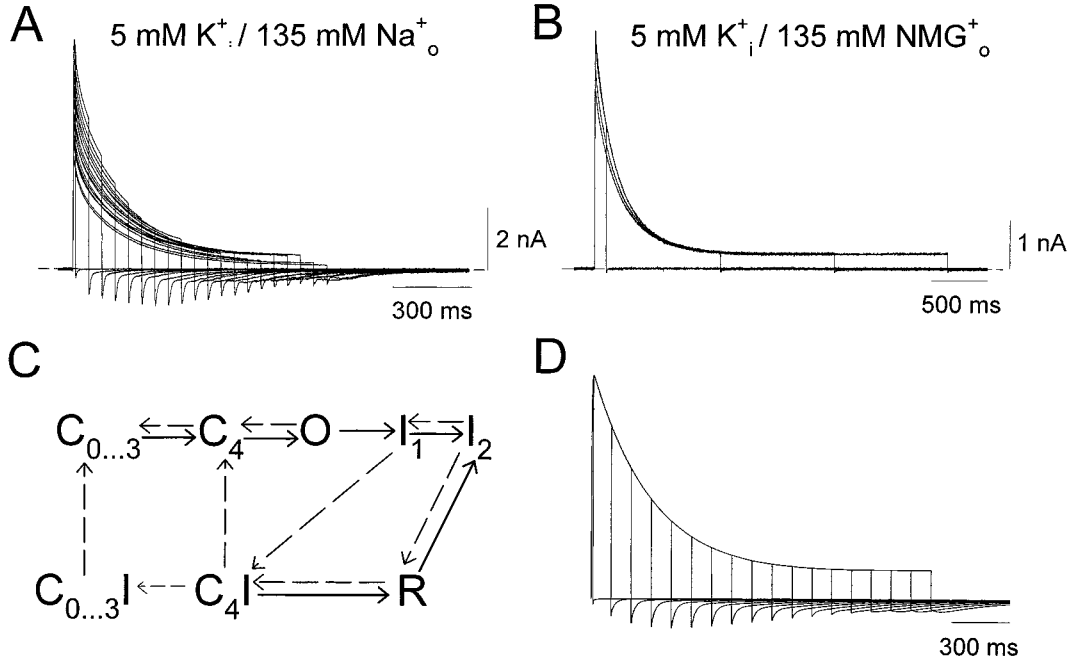

FIGURE 13 Effect of 5 mM K_i^+ on inward Na^+ tail currents. (*A*) Experimental data obtained using pulses of increasing duration from −80 to +60 mV every 20 s. The pipette contained 135 mM NMG_i^+ + 5 mM K_i^+. The decrease in outward current for later depolarizations reflects accumulated inactivation even at such a low pulse rate. (*B*) As in *A*, except that Na_o^+ was replaced by NMG_o^+. (*C*) Modification of the model of Na^+ permeation through Kv1.5 incorporating two states in the inactivation pathway. Rates were 0.003 ms^{-1} and 0.002 ms^{-1} for the O to I_1 and I_1 to I_2 transitions, respectively. Rates for the I_2 to R transition and the I_1 to C_4I transition were 0.05 ms^{-1} and 0.003 ms^{-1}, respectively. All other rates were unchanged from the model in Fig. 10. Solid and dashed arrows denote, respectively, transitions dominant at positive (+60 mV) and negative (−80 mV) potentials. (*D*) Model simulation of data presented in *A*, using the scheme presented in *C*.

model, that is somewhat different from those observed in the presence of Na_i^+ alone (Figs. 2 and 11). The slow tails on repolarization arise on the shoulder of the decaying fast tail current, and it is only after long depolarizations, when almost all channels are in the inactivated state, that a significant rising phase is observed in the slow tail current. However, it is important to note that the state R is still required in the recovery pathway to reproduce the biexponential decay of early test pulse currents, as shown in Figs. 2–4 and modeled in Fig. 11 *B*.

SUMMARY

We have seen that Kv1.5 channels can show a steady-state Na^+ conductance after entering the C-type inactivated state and that this can generate slow Na^+ tail currents with a rising phase and slow decay while recovering from the inactivated state (see above). Our observations indicate that on repolarization the inactivated channels undergo transition to an intermediate state, R, that has a higher Na^+ conductance than the inactivated channels to generate the rising phase of the slow Na^+ tail and the slowly decaying supernormal test pulse currents. Two entry pathways to the inactivated state are required to explain the biexponential decay of test pulse currents, and this is achieved through the C_4-O-I and C_4I-R-I pathways. The time course of recovery to normal closed states from closed inactivated states close to the open state can be modulated by the concentration of extracellular Na^+. This last feature suggests a general property of cations to regulate the recovery rate of K^+ channels from inactivation.

This work was supported by grants from the Heart and Stroke Foundations of British Columbia and Yukon and the Medical Research Council of Canada to DF.

REFERENCES

Aiyar, J., J. M. Withka, J. P. Rizzi, D. H. Singleton, G. C. Andrews, W. Lin, J. Boyd, D. C. Hanson, M. Simon, B. Dethlefs, C. L. Lee, J. E. Hall, G. A. Gutman, and K. G. Chandy. 1995. Topology of the pore-region of a K^+ channel revealed by the NMR-derived structures of scorpion toxins. *Neuron.* 15:1169–1181.

Aldrich, R. W., D. P. Corey, and C. F. Stevens. 1983. A reinterpretation of mammalian sodium channel gating based on single channel recording. *Nature.* 306:436–441.

Barry, D. M., J. S. Trimmer, J. P. Merlie, and J. M. Nerbonne. 1995. Differential expression of voltage-gated K^+ channel subunits in adult rat heart: relation to functional K^+ channels. *Circ. Res.* 77:361–369.

Bezanilla, F., and C. M. Armstrong. 1972. Negative conductance caused by entry of sodium and cesium ions into the potassium channels of squid axons. *J. Gen. Physiol.* 70:549–566.

Block, B. M., and S. W. Jones. 1996. Ion permeation and block of M-type and delayed rectifier potassium channels. *J. Gen. Physiol.* 107:473–488.

Bretschneider, F., A. Wrisch, F. Lehmann-Horn, and S. Grissmer. 1999. External tetraethylammonium as a molecular caliper for sensing the shape of the outer vestibule of potassium channels. *Biophys. J.* 76: 2351–2360.

Callahan, M. J., and S. J. Korn. 1994. Permeation of Na^+ through a delayed rectifier K^+ channel in chick dorsal root ganglion neurons. *J. Gen. Physiol.* 104:747–771.

DeBiasi, M., Z. Wang, E. Accili, B. Wible, and D. Fedida. 1997. Open channel block of human heart hKv1.5 by the β-subunit hKvβ1.2. *Am. J. Physiol. Heart Circ. Physiol.* 272:H2932–H2941.

Dixon, J. E., and D. McKinnon. 1994. Quantitative analysis of potassium channel mRNA expression in atrial and ventricular muscle of rats. *Circ. Res.* 75:252–260.

Doyle, D. A., J. M. Cabral, R. A. Pfuetzner, A. L. Kuo, J. M. Gulbis, S. L. Cohen, B. T. Chait, and R. MacKinnon. 1998. The structure of the potassium channel: molecular basis of K^+ conduction and selectivity. *Science.* 280:69–77.

Fedida, D., N. Maruoka, and S. Lin. 1999. Modulation of slow inactivation in human cardiac Kv1.5 channels by extra- and intra-cellular permeant cations. *J. Physiol. (Camb.).* 515:315–329.

Fedida, D., B. Wible, Z. Wang, B. Fermini, F. Faust, S. Nattel, and A. M. Brown. 1993. Identity of a novel delayed rectifier current from human heart with a cloned K^+ channel current. *Circ. Res.* 73:210–216.

French, R. J., and J. B. Wells. 1977. Sodium ions as blocking agents and charge carriers in the potassium channel of the squid giant axon. *J. Gen. Physiol.* 70:707–724.

Grissmer, S., and M. Cahalan. 1989. TEA prevents inactivation while blocking open K^+ channels in human T lymphocytes. *Biophys. J.* 55:203–206.

Hesketh, J. C., and D. Fedida. 1999. Sequential gating in the human heart K^+ channel, Kv1.5, incorporates Q1 and Q2 charge components. *Am. J. Physiol. Heart Circ. Physiol.* 274:H1956–H1966.

Hodgkin, A. L., and A. F. Huxley. 1952. The components of membrane conductance in the giant axon of Loligo. *J. Physiol. (Lond.).* 116: 473–496.

Hoshi, T., W. N. Zagotta, and R. W. Aldrich. 1991. Two types of inactivation in *Shaker* K^+ channels: effects of alterations in the carboxy-terminal region. *Neuron.* 7:547–556.

Kavanaugh, M. P., R. S. Hurst, J. Yakel, M. D. Varnum, J. P. Adelman, and R. A. North. 1992. Multiple subunits of a voltage-dependent potassium channel contribute to the binding site for tetraethylammonium. *Neuron.* 8:493–497.

Kiss, L., D. Immke, J. LoTurco, and S. J. Korn. 1998. The interaction of Na^+ and K^+ in voltage-gated potassium channels—evidence for cation binding sites of different affinity. *J. Gen. Physiol.* 111:195–206.

Kiss, L., and S. J. Korn. 1998. Modulation of C-type inactivation by K^+ at the potassium channel selectivity filter. *Biophys. J.* 74:1840–1849.

Kiss, L., J. LoTurco, and S. J. Korn. 1999. Contribution of the selectivity filter to inactivation in potassium channels. *Biophys. J.* 76:253–263.

Korn, S. J., and S. R. Ikeda. 1995. Permeation selectivity by competition in a delayed rectifier potassium channel. *Science.* 269:410–412.

Liu, Y., M. E. Jurman, and G. Yellen. 1996. Dynamic rearrangement of the outer mouth of a K^+ channel during gating. *Neuron.* 16:859–867.

Loots, E., and E. Y. Isacoff. 1998. Protein rearrangements underlying slow inactivation of the *Shaker* K^+ channel. *J. Gen. Physiol.* 112:377–389.

Lopez-Barneo, J., T. Hoshi, S. H. Heinemann, and R. W. Aldrich. 1993. Effects of external cations and mutations in the pore region on C-type inactivation of Shaker potassium channels. *Recept. Channels.* 1:61–71.

Mays, D. J., J. M. Foose, L. H. Philipson, and M. M. Tamkun. 1995. Localization of the Kv1.5 K^+ channel protein in explanted cardiac tissue. *J. Clin. Invest.* 96:282–292.

Ogielska, E. M., and R. W. Aldrich. 1998. A mutation in S6 of shaker potassium channels decreases the K^+ affinity of an ion binding site revealing ion-ion interactions in the pore. *J. Gen. Physiol.* 112:243–257.

Ogielska, E. M., and R. W. Aldrich. 1999. Functional consequences of a decreased potassium affinity in a potassium channel pore—ion interactions and C-type inactivation. *J. Gen. Physiol.* 113:347–358.

Ogielska, E. M., W. N. Zagotta, T. Hoshi, S. H. Heinemann, J. Haab, and R. W. Aldrich. 1995. Cooperative subunit interactions in C-type inactivation of K channels. *Biophys. J.* 69:2449–2457.

Panyi, G., Z. Sheng, L. Tu, and C. Deutsch. 1995. C-type inactivation of a voltage-gated K^+ channel occurs by a cooperative mechanism. *Biophys. J.* 69:896–903.

Rich, T. C., and D. J. Snyders. 1998. Evidence for multiple open and inactivated states of the hKv1.5 delayed rectifier. *Biophys. J.* 75: 183–195.

Starkus, J. G., L. Kuschel, M. D. Rayner, and S. H. Heinemann. 1997. Ion conduction through C-type inactivated *Shaker* channels. *J. Gen. Physiol.* 110:539–550.

Starkus, J. G., L. Kuschel, M. D. Rayner, and S. H. Heinemann. 1998. Macroscopic Na^+ currents in the "nonconducting" *Shaker* potassium channel mutant W434F. *J. Gen. Physiol.* 112:85–93.

Yellen, G., D. Sodickson, T.-Y. Chen, and M. E. Jurman. 1994. An engineered cysteine in the external mouth of a K^+ channel allows inactivation to be modulated by metal binding. *Biophys. J.* 66:1068–1075.

Zhu, Y., and S. R. Ikeda. 1993. Anomalous permeation of Na^+ through a putative K^+ channel in rat superior cervical ganglion neurones. *J. Physiol. (Camb.).* 468:441–461.